Since January 2020 Elsevier has created a COVID-19 resource centre with free information in English and Mandarin on the novel coronavirus COVID-19. The COVID-19 resource centre is hosted on Elsevier Connect, the company's public news and information website.

Environmental Research 196 (2021) 110947

Contents lists available at ScienceDirect

Environmental Research

journal homepage: www.elsevier.com/locate/envres

Copper-impregnated three-layer mask efficiently inactivates SARS-CoV2

Chamith Hewawaduge [a,1], Amal Senevirathne [a,1], Vijayakumar Jawalagatti [a], Jang Whan Kim [b], John Hwa Lee [a,*]

[a] College of Veterinary Medicine and Korea Zoonosis Research Institute, Jeonbuk National University, Iksan Campus, 54596, Iksan, Republic of Korea
[b] LSK Finetex Co., Ltd, Goyang-Si, Gyeonggi-Do, Republic of Korea

ARTICLE INFO

Keywords:
SARS-CoV-2
Copper sulfide
Three-layer mask
Copper mask
Cytopathy
Fluorescence
Copy number

ABSTRACT

The present study investigates the potential of SARS-CoV-2 inactivation by a copper sulfide (CuS) incorporated three-layer mask design. The mask consisted of the outer, middle, and inner layers to give comfort, strength, shape, and safety. The outer layer contained a total of 4.4% CuS (w/w) (2.2% CuS coated & 2.2% CuS impregnated) nylon fibers and the middle entrapment area contain a total of 17.6% CuS (w/w) impregnated nylon. No CuS was present in the inner layer. The antiviral efficacy assessment revealed, CuS incorporated mask is highly effective in inactivating SARS-CoV-2 within 30 min exposure. After, 1h and 2 h exposure, near-complete elimination of virus were observed by cytopathy, fluorescence, and viral copy number. The antiviral activity of the mask material was derived by incorporated solid-state CuS. Noticeably, the antiviral activity of CuS against SARS-CoV-2 was in the form of solid-state CuS, but not as Cu^{2+} ionic form derived by dissolved $CuSO_4$. The kinetics of droplet entrapment revealed, that the three-layered mask almost completely block virus-containing droplet pass-through for short exposure periods of 1–2 min, and 80% efficacy for longer exposure times of 5–10 min. We also demonstrated the incorporated CuS is evenly distributed all over the fibers assuring the uniformity of potential antiviral activity and proves, CuS particles are not easily shed out of the fabric fibers. The inactivation efficacy demonstrated against SARS-CoV-2 proves that the CuS incorporated three-layer mask will be a lifesaver during the present intense global pandemic.

1. Introduction

SARS-CoV-2, the etiological agent of the COVID-19 pandemic, was first reported in Wuhan, China (Zhu et al., 2020), during late 2019 and rapidly evolved into a global pandemic (Amanat and Krammer, 2020; Tay et al., 2020). By middle January 2021, the total global infections have passed 90 million cases with 1.9 million deaths (Johns Hopkins University, 2020). The virus is rapidly evolving into novel strains diminishing the hope shed by recent vaccines developed against SARS-CoV-2 in many countries in the world (Chung et al., 2020). Vaccine-induced complications and uncertainty have forced some populations to refuse vaccination further aggravating the situation (Khan et al., 2020; Lazarus et al., 2020). This has raised global tension and revealed the urgency of alternative approaches to contain the virus spread such as improvements in antiviral masks which can act as mechanical barriers that prevent viral contraction (Koyama et al., 2020). The present SARS-CoV-2 is a genomic relative of SARS-CoV and Middle East Respiratory Syndrome (MERS-CoV) (Petersen et al., 2020). The novel virus is highly contagious, putting the entire human population at risk of infection (Mohapatra et al., 2020). The basic reproductive rate (R0) for SARS-CoV-2 is estimated to be 2·5 (range 1·8–3·6) compared with 2·0–3·0 for SARS-CoV and the 1918 influenza pandemic, 0·9 for MERS-CoV, and 1·5 for the 2009 influenza pandemic (Petersen et al., 2020). SARS-CoV-2 is primarily transmitted between people through contact with respiratory droplets (Tang et al., 2020). The risk of infection is significantly higher if the diameter of droplets is greater than 5 μm at the time of deposition on the mucosal surfaces of the recipient (Richard et al., 2020). This new coronavirus is less deadly but far more transmissible than MERS-CoV or SARS-CoV. Because of the broad clinical spectrum and high transmissibility, timely eradication of SARS-CoV-2, as was achieved with SARS-CoV in 2003, does not seem a realistic goal. With no proven effective vaccines on the market yet, the only way to curb spread is physical distancing and the use of protective gear such as face masks to prevent the spread of the virus within the

* Corresponding author.
E-mail address: johnhlee@jbnu.ac.kr (J.H. Lee).
[1] These authors equally contributed.

https://doi.org/10.1016/j.envres.2021.110947
Received 18 October 2020; Received in revised form 23 February 2021; Accepted 25 February 2021
Available online 1 March 2021

community.

As a preventive measure, the World Health Organization recommends using face masks to minimize interpersonal transmission of SARS-CoV-2 (Chu et al., 2020). Statistics demonstrate that the appropriate use of facial masks can effectively prevent the contraction of the disease, especially among medical personnel. However, improper use of masks can also be a means of increased risk, due to deposited viral particles remain alive considerably a long time and could reach the eye, respiratory, and nasal or oral mucosa through contaminated hands (Kähler and Hain, 2020; Leung et al., 2020). Such accidental exposure can be effectively prevented if antiviral properties are incorporated into mask materials. Therefore, the incorporation of a virus-killing mechanism into mask material could be critically important to contain viral spread in the present pandemic situation. In 2008, the Environmental Protection Agency of the United States recognized copper as the first safe antiviral-antibacterial metal ion for use in human safety equipment (Grass et al., 2011). The antiviral effect of Cu^{1+} ions has been well documented (Grass et al., 2011; Gross et al., 2019). A recent study reported that when SARS-CoV-2 and SARS-CoV-1 in aerosol form were exposed to copper metallic surfaces, complete viral inactivation was observed after 4–8 h of exposure respectively (Van Doremalen et al., 2020). The antiviral properties of copper are due to the increased oxidative stress caused by reactive oxygen species and damages biomolecules (Cervantes-Cervantes et al., 2005). The virucidal activity of these ions may damage viral lipid membranes and nucleic acids, leading to inactivation (Ishida, 2018). The virucidal property may be an attribute of both Cu^{1+} and Cu^{2+} solid-state substances according to recent studies. The SARS-CoV-2 was inactivated by 99.9% in 1 h when exposed to Cu_2O coated glass surfaces (Behzadinasab et al., 2020), whereas 99.8% and 99.9% inactivation efficacy was observed for CuO coated solid surface in 30 min and 1 h exposure respectively (Hosseini et al., 2021). A few reports have demonstrated Cu^{2+} oxidative state in the form of CuS nanoparticles has demonstrated significant levels of antiviral properties against human Norovirus-like particles (Broglie et al., 2015; Cortes and Zuñiga, 2020). However, potential attributions of Cu^{2+} or S^{-2} were not elaborated. On contrary, solid-state CuS was unable to inactivate bacteriophages that are non-enveloped viruses (Sunada et al., 2012). In the present context, we elaborate and demonstrate; CuS confers superior anti-viral activity against tested enveloped viruses such as SARS-CoV-2 (beta corona) and porcine epidemic diarrhea virus (PEDV; alpha corona) but not against non-enveloped viruses such as *Salmonella* phage P22. In this study, we evaluate the antiviral effect of CuS and its application in the development of antiviral masks targeting to prevent SARS-CoV-2 transmission. Furthermore, copper substances are cheap and affordable for both developed and developing countries. The copper incorporated fabric did not have any adverse effects on the skin (Borkow and Gabbay, 2004), and therefore face masks with anti-viral and self-sterilizing properties related to copper should not pose any health hazard to the user.

Surgical-grade masks can effectively prevent the spread of airborne droplets in the clinical context. However, three-layer surgical masks with multiple nonwoven layers have the risk of becoming contaminated with droplets where the virus could still penetrate the protective layers through spaces (Zhou et al., 2020). Thus, it may not be the ideal solution for community use. During handling of masks, the hands can be contaminated with a virus, which can easily be transferred to the mucous membranes of the face. A recent study has shown that SARS-CoV-2 present on the outer surface of surgical masks can remain viable and infectious even after 6 days. According to the International Council of Nurses (ICN) ("International Council of Nurses (ICN). (2020). https://www.icn.ch/news/more-600-nurses-die-covid-19-worldwide. Called on June 10," n.d.), approximately 7% of all confirmed cases within healthcare personnel have been attributed to this route. Thus, conventional surgical masks cannot guarantee reliable protection against aerosolized droplets containing SARS-CoV-2. Hence it is pragmatic to improve the performance of face masks to minimize the risk of viral transmission through contaminated surfaces. Previous attempts were made by embedding organic and inorganic materials with nonwoven or fabric materials, and were proven to improve the antiviral effects of face masks (Zhou et al., 2020) by reducing exposure to SARS-CoV-2 to below the minimal infectious dose for an average person. Appreciable levels of SARS-CoV-2 inactivation were reported with an array of metallic substances including copper, silver, and gold where some of them were incorporated in the mask manufacturing (Balagna et al., 2020; Medhi et al., 2020).

The use of CuS as an antiviral substance and its application in protective mask manufacturing against SARS-CoV-2 is a novel initiative. This study potentially could be the first attempt of CuS incorporated mask is tested against SARS-CoV-2. To enhance the entrapment efficiency of the mask construct, it was designed in a three-layer structure with a rough outer layer, a thick middle layer with spirally arranged interwoven fabric material, and a finer interwoven inner layer. The outer and middle layers contain CuS treated fibers (either coated or impregnated) and the inner layer is completely free from CuS. The idea is to efficiently trap tiny aerosolized droplets in the middle layer where the CuS particles can inactivate viral particles. The present study demonstrates the antiviral potential of CuS treated three-layer mask and the capture efficacy by direct blocking of tiny droplets present in the air. We also elucidate the difference between solid-state CuS and ionic Cu^{2+} and the effect of CuS on enveloped viruses such as SARS-CoV-2. This study introduces CuS as a potential and effective antiviral material that can be used to produce antiviral masks which can play a significant role in preventing SARS-CoV-2 community spread during the present tensed situation caused by the pandemic.

2. Methods

2.1. Virus and cells

Vero E6 cells were obtained from the American Type Culture Collection (ATCC CRL-1586) and maintained at 37°C with 5% CO_2 in Dulbecco's modified Eagle's medium (DMEM, Lonza, Walkersville, MD, USA), supplemented with 10% heat-inactivated fetal bovine serum (FBS, Serana, Dorfstrasse, Pessin, Germany) and 1 × antibiotic-antimycotic solution (Gibco, Waltham, MS, USA). Cells were seeded in 12-well plates at a density of 1 x 10^5 cells/well and allowed to reach 70% confluence. SARS-CoV-2 (BetaCoV/Korea/KCDC 03/2020) was provided by the Korea Centers for Disease Control and Prevention (KCDC) and was propagated in Vero E6 cells. Porcine epidemic diarrhea virus (PEDV-SM98 strain) was propagated in Vero E6 cells as described previously (Hofmann and Wyler, 1988). The P22 phage, ATCC 97540 was propagated on the *Salmonella* Typhimurium ATCC 14028. All experiments using SARS-CoV-2 were performed in Korea Zoonosis Research Institute at Jeonbuk National University using enhanced biosafety level 3 (BSL3) containment procedures in KCDC approved laboratories.

2.2. Fabrication of antiviral mask

Manufacturing of CuS treated masks were conducted by LSK Finetex Co., Ltd (Goyang-Si, Gyeonggi-Do, Korea) following industrial standards. Copper sulfide solid substance coating or impregnations was done during the thread manufacturing. The CuS treatment was carried out in nylon, due to the easiness of CuS solid incorporation. The antiviral mask was designed containing three fabric layers with different fiber organizations to increase the strength, stability, shape, and particle entrapment efficacy (LSK-39260). The inner layer of the three-layer mask is a combination of 75 Denier (D) polyester, and 20 D spandex were horizontally organized to retain the shape and stability. The middle layer acted as the major entrapment area and contained 17.6% (w/w) CuS-impregnated 70 D nylon, and 75 D polyester, and 20 D spandex. The fibers in this area provided a 3D structure due to vertically organized spiral fibers. The outer layer comprised of 70 D nylon, 75 D polyester,

and 20 D spandex where the fibers were arranged in a stripe form to increase the adhesion between materials. The outer layer consisted of both CuS coated 2.2% (w/w) and 2.2% CuS impregnated nylon fibers. Each mask layer consisted of 23.2% outer layer, 52.8% middle layer, and 24% inner layer on a weight basis. For comparison purposes, the same mask construct was developed without incorporating CuS powder. Another test control with mask fibers was generated by separating the topmost layer which contained CuS coated (2.2%) and impregnated (2.2%) fibers to assess the effect of a monolayer on SARS-CoV-2 inactivation. The middle layer was inseparable because the fibers are interwoven with upper and lower layers.

2.3. Contact exposure of SARS-CoV-2 on mask materials

Three-layer mask fabric material, consisting of the outer, middle, and inner layers (LSK-39260) were prepared with and without CuS treatments. Each fabric material was cut into circular 20 mm disks that can be fit into 12 well-plates. As an experimental control, the outer top layer containing fibers of CuS coated and CuS impregnated was detached from the three-layered mask and used to assess the antiviral activity. Each fabric was then placed in 12-well plates in triplicate. To assess the inactivation efficacy of SARS-CoV-2, the viral suspension was prepared at 0.1 MOI, 35 μl was placed on the center of each textile material in the 12-well plates. Each well was then supplemented with 465 μl of serum-free DMEM to allow viral particles to be well-dispersed throughout the fabric material and incubated for 30 min, 1 h, and 2 h at 37 °C in a 5% CO_2 atmosphere. After each incubation period, textile membranes were thoroughly washed with the medium in the well, and the supernatant medium was fully collected. To get the total medium entrapped in the fabric, the remaining fabric was centrifuged in a falcon tube and the collected medium was added into the respective sample collect. The viral activity that remained in the supernatant collections was assessed by cytopathy observation, immunofluorescence, and determining the viral copy number using *in vitro* assays. Each test condition of, (1) No virus, (2) Virus alone, (3) Mask wash (washout of the CuS-mask fabric without viruses) (4) No CuS monolayer, (5) With CuS monolayer, (6) No CuS three-layered, and (7) With CuS three-layered conditions were compared.

2.4. Cytopathic effect

The cytopathic effect of SARS-CoV-2 exposed to CuS treated/or non-treated mask materials was evaluated in cultured Vero E6 cells. The cells were seeded in 12-well plates using DMEM supplemented with 10% FBS complete medium at a density of 1 x 10^5 cells/well and grown overnight at 37 °C in a humidified 5% CO_2 atmosphere. Copper membranes were infected with SARS-CoV-2 at a 0.1 multiplicity of infection (MOI) and incubated for 30 min, 1 h, and 2 h (previously described). After each infection period, the membranes were thoroughly washed with a total of 500 μl of DMEM and fully collected for infection of Vero E6 cells. The monolayers were incubated with the virus-containing serum-less medium for 1 h for infection and replenished with 4% FBS containing medium. Cells were then incubated at 37 °C in a humidified 5% CO_2 atmosphere for three to five days. Cells were observed daily for the induction of cytopathic effect using a microscope and images were taken 3 days post-infection (DPI).

2.5. 5. Immunofluorescence assay

To confirm the viability of viral particles after exposure to copper mask materials, an immunofluorescence assay was performed using infected Vero E6 cells. The monolayer of Vero E6 cells was infected with collected SARS-CoV-2 as described above. On 3 DPI, cells were fixed in 80% cold acetone for 30 min. Cells were treated with 0.1% Triton X 100 prepared in PBS, for 10 min at room temperature and washed 3 times with PBS. The cells were then incubated overnight at 4 °C with the primary antibody (SARS-CoV-2 S protein, Sino Biological) at 1:500 dilution. After incubation, the cells were washed 3 times with PBS, and FITC-labeled Alexa fluor anti-rabbit secondary antibody (Invitrogen, Carlsbad, CA, USA) was added at 1:5000 dilution followed by further incubation for 1 h in the darkness at 37 °C. Fluorescence was observed under an inverted fluorescence microscope using an appropriate channel for green fluorescence (Leica, Wetzlar, Germany).

2.6. Quantitative real-time PCR

Quantitative measurements of reduction in viral copy number were determined by the RT-PCR method after 3 DPI in the infected cell cultures. The viral RNA was isolated from infected cells using a commercial viral RNA isolation kit (Takara, Tokyo, Japan). The isolated RNA was converted into cDNA by a cDNA synthesis kit (Elpis Biotech, Daejeon, Korea) according to the manufacturer's recommendations. RT-PCR was conducted in the Applied Biosystems RT-PCR machine (Waltham, MA, USA). The PCR conditions were initial denaturation at 94°C for 3 min, followed by 40 cycles of 94°C for 20 s, 54°C for 20 s, and 72°C for 30 s. The acquired CT values were used to determine the viral copy number relying on a calibration curve developed between CT value and known copy numbers of a standard plasmid cloned with the target nuclear capsid gene (Guo et al., 2014). The primer sequences specific for the nucleocapsid gene of SARS CoV-2 viruses used for analysis were forward: CACATTGGCACCCGCAATC, reverse GAGGAACGAGAAGAGG CTTG.

2.7. Viral inactivation by copper sulfide

The viral inactivation potential of solid-state CuS and Cu^{2+} ionic form was compared by direct inoculation into SARS-CoV-2 viral particles. Copper sulfide was taken 5%, 10%, 15%, and 20% w/v in serum-free DMEM and 500 μl of each suspension was placed in 12-well plates in triplicates. Each suspension was directly inoculated in the viral cultures containing the same 0.1 MOI titer in 35 μl medium as used in the mask study. After incubating viral and CuS suspension for 30 min, 1 h, and 2 h durations, each volume was centrifuged at high speed in a tabletop centrifuge for 10 min. Then, the supernatant was collected, filtered through 0.2 μm disk filters, and used to infect Vero E6 cells for 1 h. Then, 4% FBS containing medium was added allowed to grow for 3 day at 37 °C in a 5% CO_2 atmosphere. The cytopathy, fluorescence, and viral copy numbers were determined as described above. For comparison, the ionic form of Cu^{2+} derived from $CuSO_4$ was used in 5, 10, 15, and 20 mM concentrations, and the viral inactivation was assessed similarly to CuS. The level of inactivation was assessed by observing cytopathy on Vero E6 cells. In addition, the antiviral activity of solid-state CuS on non-enveloped viruses was determined by using *Salmonella* phage P22. Here, 1%, 5%, 10%, and 20% CuS (w/v) interacted for 30 min, 1 h, and 2 h durations with phage stock, and a dotting assay was conducted to determine the titer (Bandara et al., 2012). Briefly, 0.4% soft agar was mixed with 100 μl host bacterium *Salmonella* Typhimurium ATCC14028 (mid-log phase culture) and overlaid on Luria Bertani (LB, Difco; Sparks, MD, USA) agar plates and kept 10 min for solidification. Then inactivated phage stocks were serially diluted and a 5 μl drop from each dilution was placed on soft agar. Plates were incubated at 37 °C until the plaque formation is visible in 5–6 h.

2.8. Droplet entrapment efficacy

To determine the capture efficacy of the three-layer mask structure against the mask absent conditions, a simple suction device was constructed as demonstrated in Fig. 3a. The device consisted of a small tabletop humidifier, collection chamber, mask holder, a virus collection tube, and a suction pump. The suction rate was kept constant and low during the experiment. A viral titer of 1.0 MOI was placed in the humidifier chamber and operated for 10 min for equilibration. When the

medium is disposed of in the outlet, the experiments were initiated by entrapping mask fabric in the suction cup. After, 1 min, 2 min, 5 min, and 10 min, the passed-through viral titer was determined in the 10 ml culture medium in the virus collection tube. For comparison purposes, viral pass through in (1) absence of mask material, (2) CuS treated three-layer mask material, and (3) mask without CuS was tested. The passed through viral numbers were determined by TCID50 using Vero E6 cells. Due to restrictions in SARS-CoV-2 aerosol use, here we used porcine epidemic diarrhea virus (PEDV) instead of SARS-CoV-2. The reduction in TCID50 and relative entrapment was determined by "Viral TCID50 in the presence of mask/viral TCID50 in absence of mask x 100".

2.9. Scanning electron microscopy

The morphological appearance of CuS coated and impregnated fibers were compared by scanning electron microscopy. A small amount of each fiber material was mounted on slides and coated with a conductive material. Surface scanning was done using Supra 40VP Gemini scanning electron microscopic system (Zeiss, Oberkochen, Germany) AT 10 kV acceleration voltage.

2.10. Iodometric titration for Cu^{2+} determination

To examine the leach-out of CuS or Cu^{2+} ions iodometric titration was conducted (Hammock and Swift, 1949). Two grams of three-layer mask material with and without CuS was weighed cut into small pieces and thoroughly washed with 10 ml of Milli Q distilled water. Five ml of concentrated HNO_3 was added allowed to digest for 30 min. Then concentrated ammonia solution was added drop by drop and the formation of deep blue color was observed. As a control, 2 mM $CuSO_4$ was tested. When the deep blue color appeared, the concentrated acetic acid was added drop by drop until the color disappears. At this time excess potassium iodide was added and kept in the darkness for 15 min. The amount of generated iodine was determined by titrating with 0.05 M sodium thiosulfate at the presence of a starch indicator.

2.11. Statistical analysis

Data analysis was performed using GraphPad Prism 6.02. Statistical significance was analyzed by one-way analysis of variance (ANOVA) and Student's t-test. A P value of 0.05 or less was considered statistically significant.

3. Results and discussion

3.1. Design of face masks and organization of textile layers

The most important aspect of a protective facial mask for SARS-CoV-2 prevention is how well the mask can contain aerosolized droplets generated by the user or nearby persons. Mask design should be ergonomically fit and user-friendly for comfortable and prolonged wearing throughout the day. To increase comfort, the present textile used in mask fabrication maintains strength, shape, and stability. To increase droplet entrapment efficacy, the mask barrier was designed in three layers, consisting of an outer layer fabricated using 2.2% w/w CuS coated and 2.2% w/w CuS impregnated 70D nylon fibers, 75D polyester, and 20D spandex arranged in a stripe form to increase adhesion. The fibers in the thicker middle layer are spirally arranged, and consists of polyester and 17.6% w/w CuS impregnated 70D nylon and 75D polyester, 20D spandex fibers were arranged in a supercoiled and vertical orientation for enhanced entrapment. The innermost layer is soft and does not contain any CuS. A hundred grams of the complete three-layer mask material contains, 23.2 g; the outer layer, 52.8 g; the middle layer, and 24 g; the inner layer on a weight basis. The total composition of CuS thread in a mask is 22 g per 100 g of total weight. The outer and middle layers were incorporate with CuS mediated antiviral properties, so the user is protected from the deposited viral contaminants from the outside environment.

3.2. Inhibition of viral activity upon exposure to copper-treated mask materials

The architecture and the concentration of copper compounds are the key parameters affecting entrapment and inhibition of viral activity. To investigate the inactivation efficacy of a complete three-layer mask against SARS-CoV-2, a known viral titer (0.1 MOI) was allowed to interact with the mask material, with and without CuS treatment for variable durations, 30 min, 1 h, and 2 h. For comparison purposes, a detached top layer of mask materials, with and without CuS treatment was also investigated. No virus condition, virus alone condition, and mask wash-through without viruses were kept as test controls. After incubation, viral particles available on fabric material were thoroughly washed with culture medium (DMEM, 2% FBS) and fully collected by the pipette and by centrifugation. The level of viral inactivation was assessed by infecting Vero E6 cell monolayers. Cells were incubated for 3–5 days and the cytopathy was evaluated on daily basis. The cytopathy observation revealed a significant level of cell protection in both CuS treated three-layer mask and monolayered conditions. Comparison of inactivation times revealed, even 30 min exposure brings a significant level of SARS-CoV-2 inactivation when they are exposed to CuS containing three-layer mask material. After 1 h and 2 h exposure times, the CuS treated three-layer mask derived almost complete protection with perfectly intact cells. Cells in all treatments that do not contain CuS resulted in profound cell death at all time points. The detached outer layer consists of CuS also significantly protective against SARS-CoV-2 proving that even monolayer can significantly inactivate SARS-CoV-2 after 1 h and 2 h durations (Fig. 1a). Furthermore, the wash through of CuS treated mask fabric did not cause any cytopathy or visible damage on Vero E6 cell monolayers, confirming the antiviral effect is coming from solid-state CuS (Fig. 1a) but not by the fiber itself. The results of cytopathy could be further corroborated by immunofluorescence assay, which revealed significant intracellular viral activity in non-CuS treated mask conditions, irrespective of the mask structure, whether it is three layered or monolayered (Fig. 1b) mask material. The emission of fluorescence was completely absent from cells incubated with virus collected from the three-layer mask for all time points confirming significant SARS-CoV-2 inactivation occur as early as 30 min. And the comparable results were obtained for CuS treated monolayer for 1 and 2 h time points. When determining the viral copy numbers, all treatments containing CuS three-layer masks resulted in the lowest numbers in all three-time points. Whereas the CuS containing mask top layer demonstrate a time-dependent pattern of inactivation with significant inhibition after 1 and 2 h. All mask materials without CuS treatment unable to show a significant reduction in viral copy number, ensuring that the observed antiviral activity can be attributed to solid-state CuS embodied into the mask fabrication (Fig. 1c).

3.3. Viral inactivation capacity of solid-state CuS

The antiviral properties of solid-state CuS are less investigated. Very few reports could be found concerning the antiviral properties of CuS (Broglie et al., 2015). To elaborate on antiviral properties demonstrated by solid-state CuS, we conducted a study by directly inoculating SARS-CoV-2 into a medium containing CuS. Variable concentrations of CuS substance were incorporated into known viral titer of 0.1 MOI, at 5%, 10%, 15%, and 20% CuS w/v concentration and incubated for 30 min, 1 h, and 2 h. Examination of viral inactivation by cytopathy (Fig. 2a), fluorescence (Fig. 2b), and viral copy numbers (Fig. 2c) revealed dose and time-dependent inactivation pattern is present with CuS. In contrast to CuS solid material, Cu^{2+} ions derived by dissolving $CuSO_4$ did not show any appreciable level of viral inactivation even at increased molarity levels or increased incubation times (Supplementary

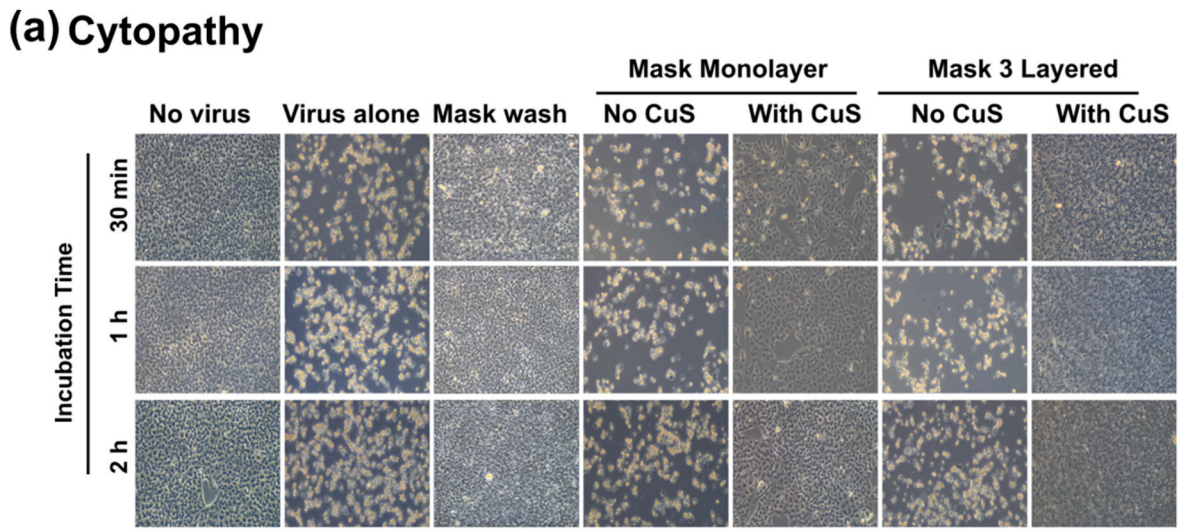

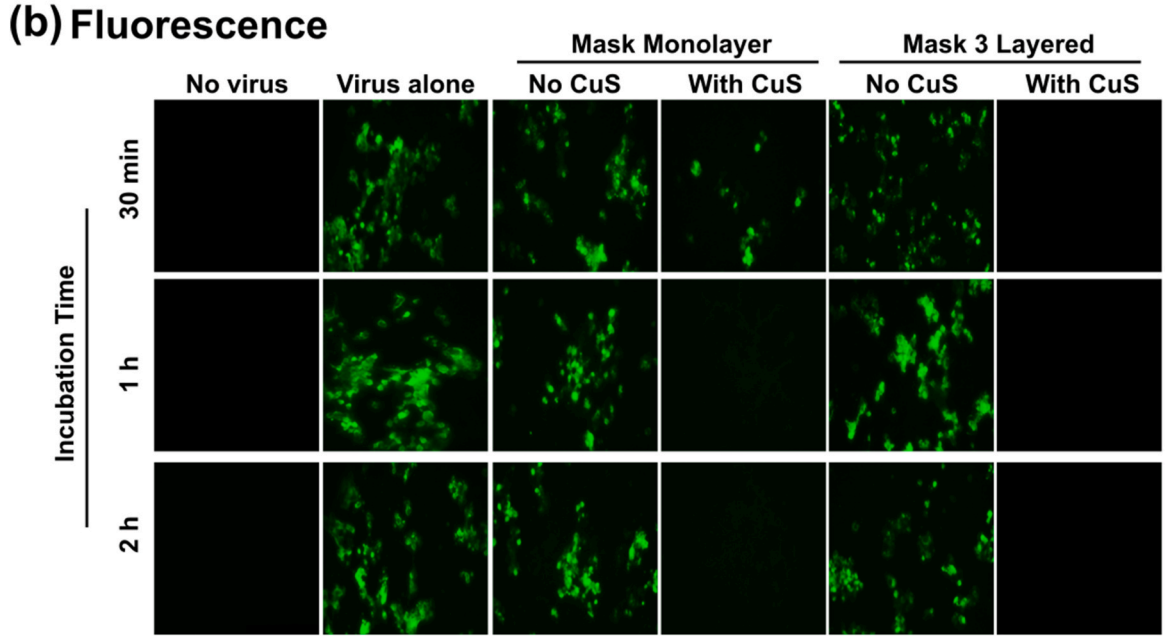

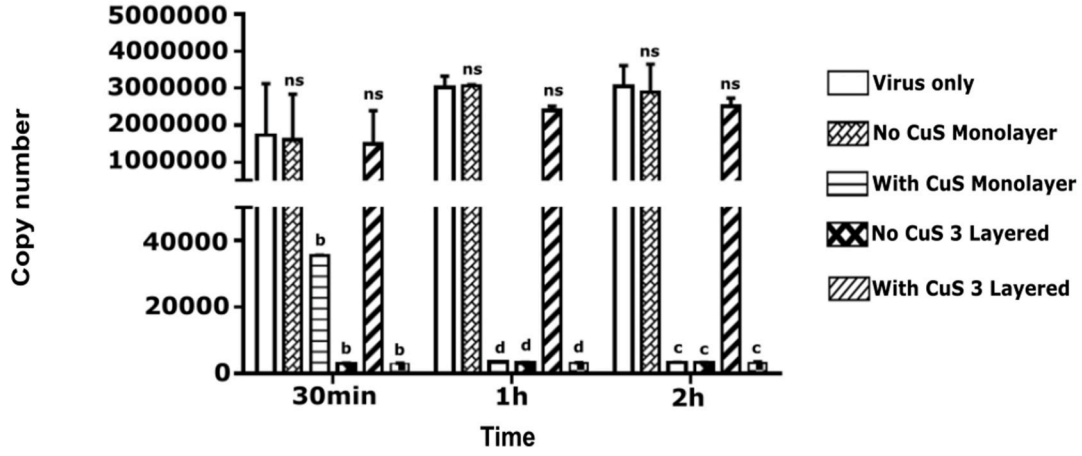

(caption on next page)

Fig. 1. Inhibition of SARS-CoV2 replication by CuS incorporated three-layer mask fabrics. A known titer of SARS-CoV-2 interacted with mask materials and inactivation after 30 min, 1 h, and 2 h exposure times were evaluated. (a) Cytopathic effect (CPE). The CPE was evaluated in Vero E6 cells after 3 DPI. The CPE on (1) No virus, (2) Virus alone, (3) Mask wash (wash through of CuS-mask material without virus), (4) No CuS monolayer (outer layer of the mask), (5) With CuS monolayer (outer layer of the mask), (6) No CuS 3 layered mask, and (7) With CuS 3 layered mask were compared. No CPE was observed in the virus incubated with 3 layered CuS incorporated mask material, whereas typical CPE characteristics, cell rounding, and syncytium formation were observed in SARS-CoV2 incubated with no copper mask fabric material. (b) Fluorescence microscopy. Upon virus incubation with mask materials with or without copper sulfide were assessed at 3 DPI, the cells were fixed and incubated with SARS-CoV-2 S protein-specific antibody as primary and with FITC-labeled Alexa fluor as the secondary antibody. Three-layered mask generated no fluorescence and comparable to no virus controls in all time points. (c) RT-qPCR analysis of viral replication inhibition in Vero E6 cells after incubation with mask fabric materials with or without copper sulfide. Each value was expressed as the mean ± SEM (n = 2). $^{b}P < 0.01$, $^{c}P < 0.001$, and $^{d}P < 0.0001$ compared to the virus only group. ns: no significant, dpi: days post-infection.

Fig. 1). This suggests that the currently observed antiviral effect must be a property of CuS solid-state substance, but not with the ionic form of Cu^{2+} ions. Interestingly CuS solid substance did not show any antiviral activity against bacteriophages as demonstrated by incubation with *Salmonella* phage P22 (Sunada et al., 2012). No reduction in phage titers was observed with increased CuS concentration or increased time (Supplementary Fig. 2). This observation suggests that the antiviral effect of CuS could only be confounded to enveloped viruses, such as coronaviruses or influenza viruses, but not against non-enveloped viruses such as bacteriophages. This also demonstrates CuS may probably damage viral envelop making them unable to infect the host cell. Similar, antiviral activity of CuS could also be observed against the PEDV which is a type of enveloped alpha coronavirus (data are not shown). The antiviral activity observed with solid state CuS, but not with $CuSO_4$ leads to a potential argument whether sulfide ions could implicated on antiviral activity of CuS. Effect of sulfide ions also undeniable with a recently published article that has highlighted antiviral properties of hydrogen sulfide against broad spectrum of enveloped viruses (Bazhanov et al., 2017). When considering the same ionic state of copper, Cu^{2+} ions in the form of cupric oxide (CuO) reported having a little effect on influenza virus inactivation (Minoshima et al., 2016) compared to pronounced antiviral properties of cuprous oxide (Cu_2O). This background further supports the potential involvement of sulfide ions (S^{-2}). However, we observed the solubility of CuS ions in an aqueous medium is extremely low, leaving us skeptical whether a sufficient level of ionic dissociation occurs in the culture medium. Therefore more elaborated study may require fully elucidating the antiviral effect of CuS on enveloped viruses.

3.4. Entrapment efficacy

A simple device was designed to compare particle entrapment efficacy of mask material to evaluate viral exposure in conditions (1) without a mask, (2) with No-CuS mask, and (3) with CuS mask. Due to health restriction persistent to SARS-Co-V2 aerosol use, here we employed non-human host alphacoronavirus PEDV to assess the entrapment efficacy. The sterile humidifiers were filled with a medium with known viral titer at 1.0 MOI and equilibrated for 10 min. When the medium is diffused into the fume chamber, it was visible due to the color of media deposited on sidewalls. To test, short, moderate, and long exposure times, the viral pass through assessment was conducted for 1, 2, 5, and 10 min periods. Under each condition, (1) No mask, (2) with No-CuS mask, (3) With CuS mask, the viral pass through was assessed by determining the titer at virus collection tube (marked as 5) in Fig. 3a. The viral titer was determined by $TCID_{50}$. In short exposure times, both three-layer masks, irrespective of the presence or absence of CuS were able to near-complete protection compared to no mask conditions. However, when the continuous exposure continued over a 5 and 10 min period, a gradual increase in the viral titer in the collection tube could be observed that reduced the relative protection efficacy down to 80% (Fig. 3b).

3.5. Scanning electron microscopy

The surface morphological appearance of CuS coated and impregnated fibers were assessed by electron microscopy. The uniformity of particle spread and consistency fiber thickness and the possibility of detaching particles were examined. A clear difference of fiber surface could be seen between CuS coated (Fig. 4a) and CuS impregnated (Fig. 4b) fibers where the rough surface and smooth surface were visible for each coated and impregnated conditions. No signs of particle detachment were seen. Comparison of surface plot demonstrated almost even distribution of CuS on fiber material for coated fibers and a much smoother surface for impregnated fibers. Strong and consistent coating and impregnation prevent the possibility of detaching CuS particles and shed on the skin posing potential health risks that can be caused by CuS. Microscopic studies and determination of Cu^{2+} ions in the leach-out could not detect any considerable levels by iodometric titration.

3.6. Effect of mask design on inhibition of SARS-CoV-2

The results obtained from the present study suggest that the three-layer mask design is highly efficient in preventing virus pass-through during short exposure times. This is the normal spontaneous exposure that could occur in daily life. The entrapment efficacy did not affect by CuS presence or absence. The mechanical barrier efficiently and nonspecifically prevents droplet pass-through into the nasal cavity. The incorporation of CuS has created mask material that is highly proficient in inactivating highly contagious SARS-CoV-2. We hypothesize, that the solid-state CuS may damage viral envelop making them unable to infect the host cell. However, more elaborated experiments may be required to fully elucidate the mechanism of action. Viral inhibition kinetics confirmed time-dependent and dose-dependent inhibition of viral activity and the effect of mask design on efficient entrapment and inhibition. Inactivation of viral particles by the CuS containing three-layer mask was a rapid one that initiated even after 30 min. Otherwise, SARS-CoV-2 is capable to stay alive for over a week posing an immense threat to public societies. Therefore, the present CuS treated antiviral mask is an ideal remedy to prevent the spread of SARS-CoV-2 (Fig. 5). The spiral arrangement of the nylon fibers in the entrapment area is positively charged, which could also increase the capture of negatively charged viral particles (Cha M-R et al., 1993). Due to the adequate space and airflow of these compared to conventional high-efficiency particulate (HEPA) masks such as the N95, they may be easier to wear for long periods (Kim, 2020).

4. Conclusion

The data of the present study reveals CuS incorporated three-layer mask can be highly effective in inactivating SARS-CoV-2 in a short period of exposure time. The three-dimensional design efficiently blocks the virus-containing droplets pass-through demonstrating the potential use in the present pandemic. The increased surface area of three-dimensional architecture improves capture and antiviral action via the interaction of CuS with entrapped virions in the mask or that come into contact with the surface. The present copper-impregnated three-layer masks could mitigate social burdens related to the uncontrolled spread of highly contagious SARS-CoV-2 in a midst of the present global pandemic. As of the present date, the hope of an effective vaccine is still doubtful due to the rapidly evolving nature and antigenic drift of SARS-

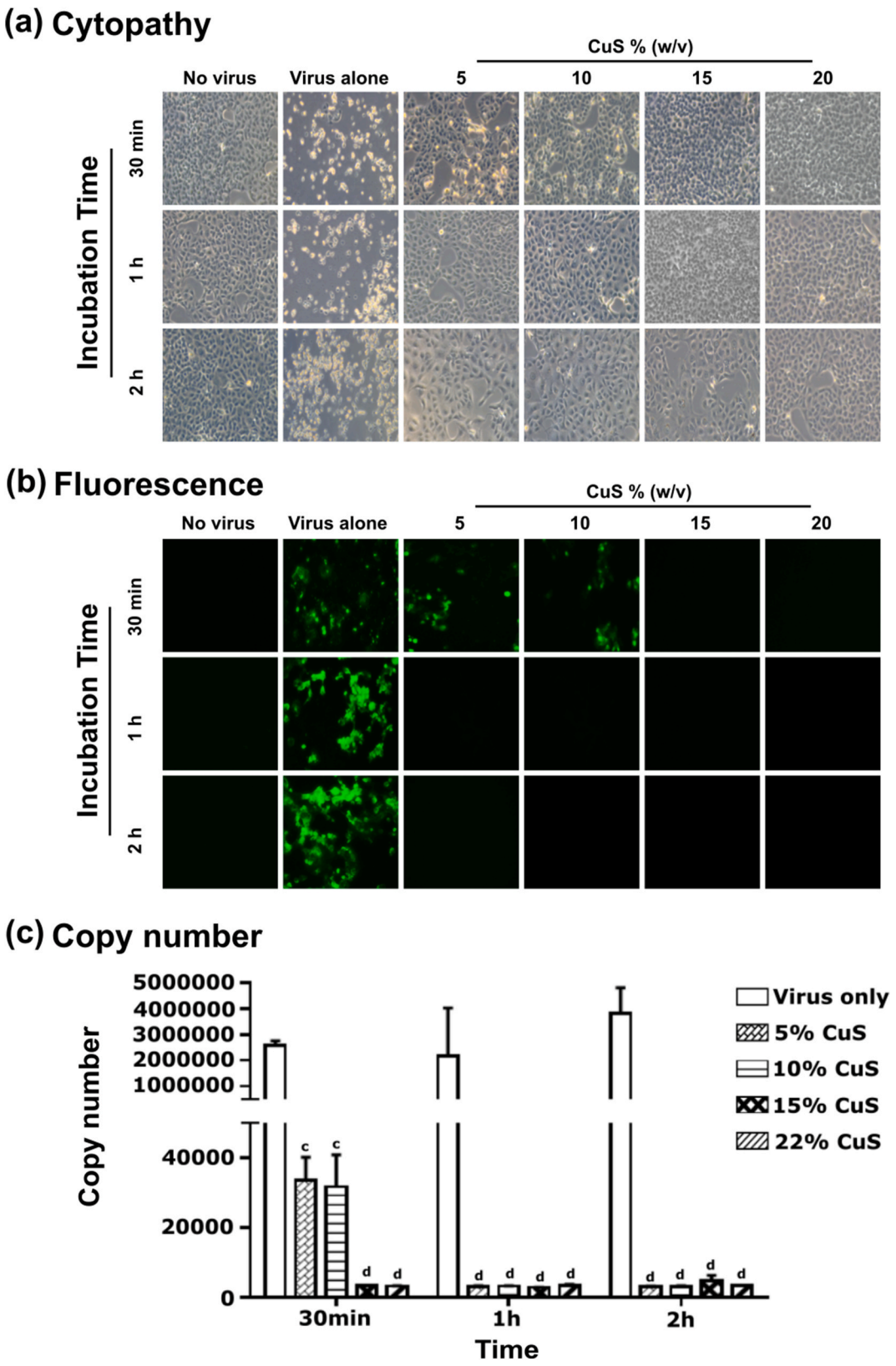

Fig. 2. The antiviral activity of CuS compound on SARS-CoV-2. (a) SARS-CoV-2 virus at 0.1 MOI was exposed to 5%, 10%, 15% and 20% (w/v) CuS. After specified 30 min, 1 h, and 2 h exposure times, the viral particles were collected and were incubated with cultured Vero E6 cells and observed for cellular cytopathic effects. At 3dpi, the degree of cellular damage was compared against non-infected control and virus alone infected controls and photographed under the bright field of an inverted microscope. (b) The inhibition effects of CuS against SARS-CoV-2 in virus co-addition treatment with CuS compound of interest at 5%, 10%, 15%, and 20% detected by immunofluorescence assay after specified 30 min, 1 h, and 2 h exposure times. (c) Quantitative real-time RT-PCR. Viral RNA was isolated from infected cell supernatants at 3 DPI, and the copy numbers were determined by quantitative Real-Time PCR (qRT-PCR) with primers targeting the N gene. Each value was expressed as the mean ± SEM (n = 2). $^{c}P < 0.001$, and $^{d}P < 0.0001$ compared to the virus only group.

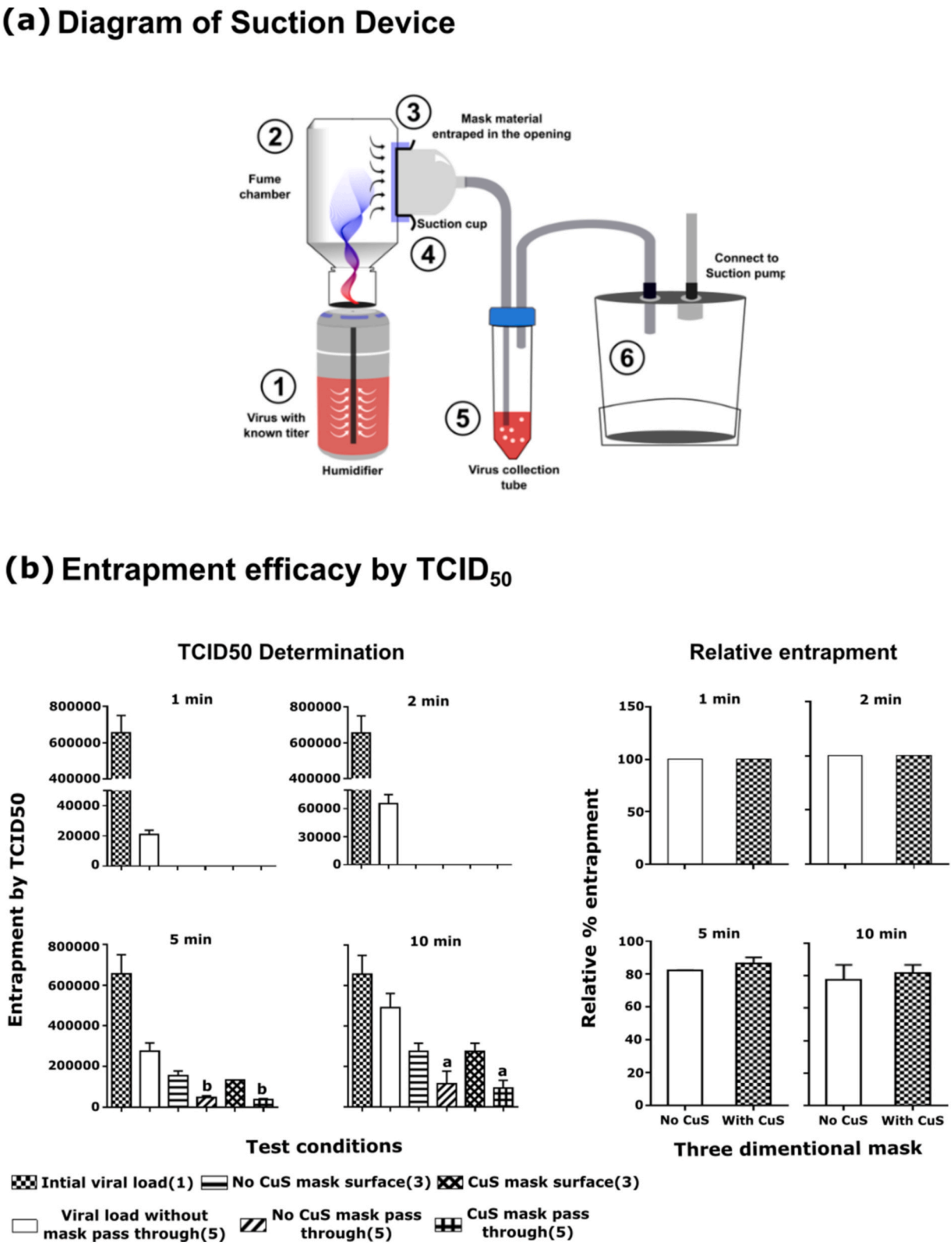

Fig. 3. Viral entrapment by mask fabric material. (a) Schematic representation of the suction device (b) Entrapment efficacy assessment by TCID50. The viral particles were allowed to pass through the opening of the suction cup with or without mask fabric attached to it. The viral particles that pass through the opening were channeled into the virus collection tube, where the titer was determined by TCID50 assessment. The relative viral entrapment efficacy was determined in comparison to non-mask condition according to the formula "Relative % entrapment = Viral titer in the collection tube with mask/Viral titer in the collection tube without mask x 100". Each value was expressed as the mean ± SEM (n = 2). $^{a}P < 0.05$, and $^{b}P < 0.01$.

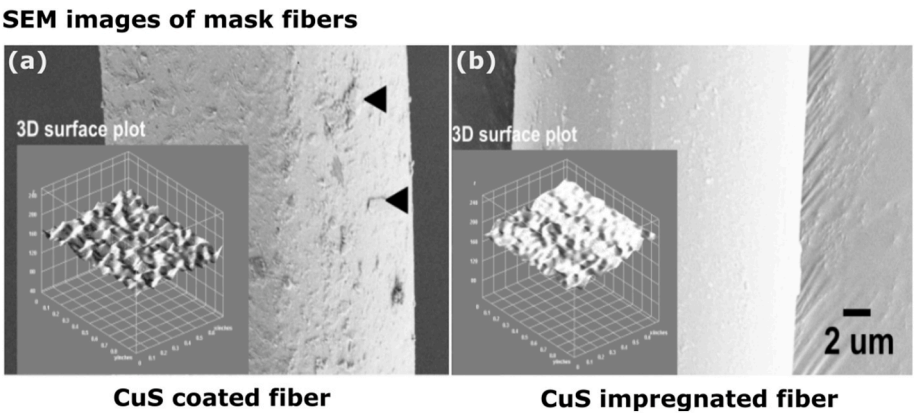

Fig. 4. Scanning electron microscopic assessment of mask fibers. (a) CuS coated and (b) CuS impregnated mask fiber. Black arrows indicate CuS particles tightly attached on the mask fiber surface of CuS coated fibers whereas the CuS impregnated mask fibers remain with a smooth surface. Intersections depict a 3D surface plot generated by Image J software.

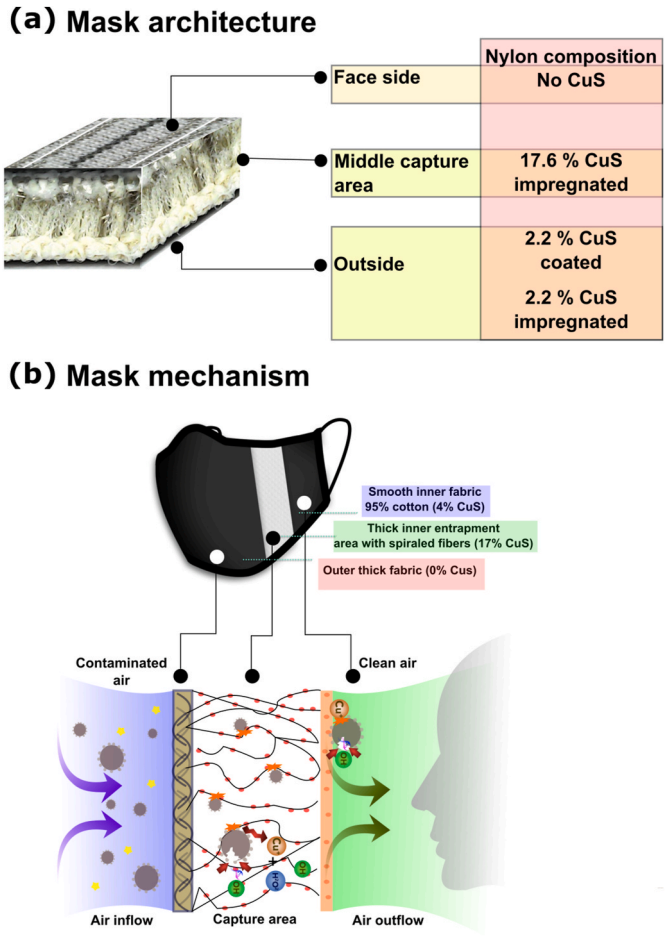

Fig. 5. Schematic representation of mask architecture and capture mechanism. (a) The arrangement of mask layers and CuS incorporated fiber composition. (b) Entrapment mechanism of the three-layer mask.

CoV-2, the development of antiviral, self-sterilizing masks will be utterly advantageous to save precious human lives by masking the viral spread and contractions within vulnerable communities.

Credit author's statement

Chamith Hewawaduge: Conceived the idea, designed and conducted experiments. Prepared the original manuscript. Amal Senevirathne: Conceived the idea, designed and conducted experiments, prepared the original manuscript, contributed to manuscript review and preparation of the final version. Vijayakumar Jawalagatti: Designed and conducted experiments. Jang Whan Kim: Three-layer mask designer, provided financial support. John Hwa Lee: Conceived the idea, contributed to manuscript review and preparation of the final version, provided financial support.

Declaration of competing interest

Authors declare that they have no conflict of interest, and all authors have agreed and approved the final manuscript.

Acknowledgment

This research was supported by Basic Science Research Program through the National Research Foundation of Korea (NRF) funded by the Ministry of Education (2019R1A6A1A03033084) and LSK Finetex Co. Ltd, Goyang-Si, Gyeonggi-Do, Korea.

Appendix A. Supplementary data

Supplementary data to this article can be found online at https://doi.org/10.1016/j.envres.2021.110947.

References

Amanat, F., Krammer, F., 2020. SARS-CoV-2 vaccines: status report. Immunity 52 (4), 583–589. https://doi.org/10.1016/j.immuni.2020.03.007.
Balagna, C., Perero, S., Percivalle, E., Nepita, E.V., Ferraris, M., 2020. Virucidal effect against coronavirus SARS-CoV-2 of a silver nanocluster/silica composite sputtered coating. Open Ceram. https://doi.org/10.1016/j.oceram.2020.100006.
Bandara, N., Jo, J., Ryu, S., Kim, K.P., 2012. Bacteriophages BCP1-1 and BCP8-2 require divalent cations for efficient control of Bacillus cereus in fermented foods. Food Microbiol. 31, 9–16. https://doi.org/10.1016/j.fm.2012.02.003.
Bazhanov, N., Escaffre, O., Freiberg, A.N., Garofalo, R.P., Casola, A., 2017. Broad-range antiviral activity of hydrogen sulfide against highly pathogenic RNA viruses. Sci. Rep. https://doi.org/10.1038/srep41029.
Behzadinasab, S., Chin, A., Hosseini, M., Poon, L., Ducker, W.A., 2020. A surface coating that rapidly inactivates SARS-CoV-2. ACS Appl. Mater. Interfaces 12 (31), 34723–34727. https://doi.org/10.1021/acsami.0c11425.
Borkow, G., Gabbay, J., 2004. Putting copper into action: copper-impregnated products with potent biocidal activities. Faseb. J. 18 (14), 1728–1730. https://doi.org/10.1096/fj.04-2029fje.
Broglie, J.J., Alston, B., Yang, C., Ma, L., Adcock, A.F., Chen, W., Yang, L., 2015. Antiviral activity of gold/copper sulfide core/shell nanoparticles against human norovirus virus-like particles. PloS One 10 (10). https://doi.org/10.1371/journal.pone.0141050.
Cervantes-Cervantes, M.P., Calderón-Salinas, J.V., Albores, A., Muñoz-Sánchez, J.L., 2005. Copper increases the damage to DNA and proteins caused by reactive oxygen

species. Biol. Trace Elem. Res. 103 (3), 229–248. https://doi.org/10.1385/BTER:103:3:229.
Cha, M.-R., Evans, M.L., Hangarter, R.P., 1993. Novel use of positively charged nylon transfer membranes for trapping indoleacetic acid or other small anions during efflux from plant tissues. Plant Physiol. Biochem. 31 (2), 263–269.
Chu, D.K., Akl, E.A., Duda, S., Solo, K., Yaacoub, S., Schünemann, H.J., El-harakeh, A., Bognanni, A., Lotfi, T., Loeb, M., Hajizadeh, A., Bak, A., Izcovich, A., Cuello-Garcia, C.A., Chen, C., Harris, D.J., Borowiack, E., Chamseddine, F., Schünemann, F., Morgano, G.P., Muti Schünemann, G.E.U., Chen, G., Zhao, H., Neumann, I., Chan, J., Khabsa, J., Hneiny, L., Harrison, L., Smith, M., Rizk, N., Giorgi Rossi, P., AbiHanna, P., El-khoury, R., Stalteri, R., Baldeh, T., Piggott, T., Zhang, Y., Saad, Z., Khamis, A., Reinap, M., 2020. Physical distancing, face masks, and eye protection to prevent person-to-person transmission of SARS-CoV-2 and COVID-19: a systematic review and meta-analysis. Lancet 395, 1973–1987. https://doi.org/10.1016/S0140-6736(20)31142-9, 10242.
Chung, Y.H., Beiss, V., Fiering, S.N., Steinmetz, N.F., 2020. Covid-19 vaccine frontrunners and their nanotechnology design. ACS Nano 14 (10), 12522–12537. https://doi.org/10.1021/acsnano.0c07197.
Cortes, A.A., Zuñiga, J.M., 2020. The use of copper to help prevent transmission of SARS-coronavirus and influenza viruses. A general review. Diagn. Microbiol. Infect. Dis. 98 (4), 115176–115180. https://doi.org/10.1016/j.diagmicrobio.2020.115176.
Grass, G., Rensing, C., Solioz, M., 2011. Metallic copper as an antimicrobial surface. Appl. Environ. Microbiol. 77 (5), 1541–1547. https://doi.org/10.1128/AEM.02766-10.
Gross, T.M., Lahiri, J., Golas, A., Luo, J., Verrier, F., Kurzejewski, J.L., Baker, D.E., Wang, J., Novak, P.F., Snyder, M.J., 2019. Copper-containing glass ceramic with high antimicrobial efficacy. Nat. Commun. https://doi.org/10.1038/s41467-019-09946-9.
Guo, H., Liu, X., Xu, Y., Han, Z., Shao, Y., Kong, X., Liu, S., 2014. A comparative study of pigeons and chickens experimentally infected with PPMV-1 to determine antigenic relationships between PPMV-1 and NDV strains. Vet. Microbiol. 168 (1), 88–97. https://doi.org/10.1016/j.vetmic.2013.11.002.
Hammock, E.W., Swift, E.H., 1949. Iodometric determination of copper. Anal. Chem. 21 (8), 975–980. https://doi.org/10.1021/ac60032a028.
Hofmann, M., Wyler, R., 1988. Propagation of the virus of porcine epidemic diarrhea in cell culture. J. Clin. Microbiol. 26 (11), 2235–2239. https://doi.org/10.1128/jcm.26.11.2235-2239.1988.
Hosseini, M., Chin, A.W.H., Behzadinasab, S., Poon, L.L.M., Ducker, W.A., 2021. Cupric oxide coating that rapidly reduces infection by SARS-CoV-2 via solids. ACS Appl. Mater. Interfaces 13 (5), 5919–5928. https://doi.org/10.1021/acsami.0c19465.
International Council of Nurses (ICN), 2020. Called on June 10, n.d. https://www.icn.ch/news/more-600-nurses-die-covid-19-worldwide.
Ishida, T., 2018. Antiviral activities of Cu 2+ ions in viral prevention, replication, RNA degradation, and for antiviral efficacies of lytic virus, ROS-mediated virus, copper chelation. World Sci. News. 99, 148–168.
Johns Hopkins University, 2020. COVID-19 Map - Johns Hopkins Coronavirus Resource Center [WWW Document]. Johns Hopkins Coronavirus Resour, Cent.
Kähler, C.J., Hain, R., 2020. Fundamental protective mechanisms of face masks against droplet infections. J. Aerosol Sci. https://doi.org/10.1016/j.jaerosci.2020.105617.
Khan, Y.H., Mallhi, T.H., Alotaibi, N.H., Alzarea, A.I., Alanazi, A.S., Tanveer, N., Hashmi, F.K., 2020. Threat of COVID-19 vaccine hesitancy in Pakistan: the need for measures to neutralize misleading narratives. Am. J. Trop. Med. Hyg. 103 (2), 603–604. https://doi.org/10.4269/ajtmh.20-0654.
Kim, M.N., 2020. What type of face mask is appropriate for everyone-mask-wearing policy amidst COVID-19 pandemič. J. Kor. Med. Sci. 35 (20) https://doi.org/10.3346/JKMS.2020.35.E186.
Koyama, T., Weeraratne, D., Snowdon, J.L., Parida, L., 2020. Emergence of drift variants that may affect covid-19 vaccine development and antibody treatment. Pathogens 9 (5), 324. https://doi.org/10.3390/pathogens9050324.
Lazarus, J.V., Ratzan, S.C., Palayew, A., Gostin, L.O., Larson, H.J., Rabin, K., Kimball, S., El-Mohandes, A., 2020. A global survey of potential acceptance of a COVID-19 vaccine. Nat. Med. 27, 225–228. https://doi.org/10.1038/s41591-020-1124-9.
Leung, N.H.L., Chu, D.K.W., Shiu, E.Y.C., Chan, K.H., McDevitt, J.J., Hau, B.J.P., Yen, H. L., Li, Y., Ip, D.K.M., Peiris, J.S.M., Seto, W.H., Leung, G.M., Milton, D.K., Cowling, B. J., 2020. Respiratory virus shedding in exhaled breath and efficacy of face masks. Nat. Med. 26, 676–680. https://doi.org/10.1038/s41591-020-0843-2.
Medhi, R., Srinoi, P., Ngo, N., Tran, H.V., Lee, T.R., 2020. Nanoparticle-based strategies to combat COVID-19. ACS Appl. Nano Mater. 3 (9), 8557–8580. https://doi.org/10.1021/acsanm.0c01978.
Minoshima, M., Lu, Y., Kimura, T., Nakano, R., Ishiguro, H., Kubota, Y., Hashimoto, K., Sunada, K., 2016. Comparison of the antiviral effect of solid-state copper and silver compounds. J. Hazard Mater. 15 (312), 1–7. https://doi.org/10.1016/j.jhazmat.2016.03.023.
Mohapatra, R.K., Pintilie, L., Kandi, V., Sarangi, A.K., Das, D., Sahu, R., Perekhoda, L., 2020. The recent challenges of highly contagious COVID-19, causing respiratory infections: symptoms, diagnosis, transmission, possible vaccines, animal models, and immunotherapy. Chem. Biol. Drug Des. 96 (5), 1187–1208. https://doi.org/10.1111/cbdd.13761.
Petersen, E., Koopmans, M., Go, U., Hamer, D.H., Petrosillo, N., Castelli, F., Storgaard, M., Al Khalili, S., Simonsen, L., 2020. Comparing SARS-CoV-2 with SARS-CoV and influenza pandemics. Lancet Infect. Dis. 20 (9), 238–244. https://doi.org/10.1016/S1473-3099(20)30484-9.
Richard, M., Kok, A., de Meulder, D., Bestebroer, T.M., Lamers, M.M., Okba, N.M.A., Fentener van Vlissingen, M., Rockx, B., Haagmans, B.L., Koopmans, M.P.G., Fouchier, R.A.M., Herfst, S., 2020. SARS-CoV-2 is transmitted via contact and via the air between ferrets. Nat. Commun. 11, 3496. https://doi.org/10.1038/s41467-020-17367-2.
Sunada, K., Minoshima, M., Hashimoto, K., 2012. Highly efficient antiviral and antibacterial activities of solid-state cuprous compounds. J. Hazard Mater. 235–236, 265–270. https://doi.org/10.1016/j.jhazmat.2012.07.052.
Tang, S., Mao, Y., Jones, R.M., Tan, Q., Ji, J.S., Li, N., Shen, J., Lv, Y., Pan, L., Ding, P., Wang, X., Wang, Y., MacIntyre, C.R., Shi, X., 2020. Aerosol transmission of SARS-CoV-2? Evidence, prevention and control. Environ. Int. 144, 106039. https://doi.org/10.1016/j.envint.2020.106039.
Tay, M.Z., Poh, C.M., Rénia, L., MacAry, P.A., Ng, L.F.P., 2020. The trinity of COVID-19: immunity, inflammation and intervention. Nat. Rev. Immunol. 20, 363–374. https://doi.org/10.1038/s41577-020-0311-8.
Van Doremalen, N., Bushmaker, T., Morris, D.H., Holbrook, M.G., Gamble, A., Williamson, B.N., Tamin, A., Harcourt, J.L., Thornburg, N.J., Gerber, S.I., Lloyd-Smith, J.O., De Wit, E., Munster, V.J., 2020. Aerosol and surface stability of SARS-CoV-2 as compared with SARS-CoV-1. N. Engl. J. Med. 382, 1564–1567. https://doi.org/10.1056/NEJMc2004973.
Zhou, J., Hu, Z., Zabihi, F., Chen, Z., Zhu, M., 2020. Progress and perspective of antiviral protective. Material. Adv. Fiber Mater. 2, 123–139. https://doi.org/10.1007/s42765-020-00047-7.
Zhu, N., Zhang, D., Wang, W., Li, X., Yang, B., Song, J., Zhao, X., Huang, B., Shi, W., Lu, R., Niu, P., Zhan, F., Ma, X., Wang, D., Xu, W., Wu, G., Gao, G.F., Tan, W., 2020. A novel coronavirus from patients with pneumonia in China, 2019. N. Engl. J. Med. 382, 727–733. https://doi.org/10.1056/NEJMoa2001017.